International Journal of Signal Processing, Image Processing and Pattern Recognition
Vol.7, No.1 (2014), pp.87-98
http://dx.doi.org/10.14257/ijsip.2014.7.1.09

Comparison of Interpolation Methods in Bayer CFA Image Compression Based on Structure Separation and APBT-JPEG

Chengyou Wang, Baochen Jiang and Hao Yuan

School of Mechanical, Electrical and Information Engineering, Shandong University, Weihai 264209, P. R. China
wangchengyou@sdu.edu.cn, jbc@sdu.edu.cn, yuanhao@sdu.edu.cn

Abstract

The color filter array (CFA) captures only one-third of the necessary color intensities and the full color image is generated from the captured data by interpolation. In recent years, the algorithm of Bayer patterned image compression based on "structure separation" has achieved better image quality. On the basis of previous work, the algorithm based on the all phase biorthogonal transform (APBT) and interpolation is proposed in this paper. Instead of the conventional DCT-JPEG, the APBT-JPEG significantly reduces complex multiplications and makes the quantization table easier. Several kinds of interpolation methods to the decompressed image data are also discussed in this paper, including nearest neighbor interpolation, bilinear interpolation, cubic convolution interpolation and a novel interpolation method based on APIDCT. Experimental results show that the proposed algorithm outperforms the one based on "structure separation"; and the APIDCT interpolation performs close to the conventional interpolation methods and behaves better than them at high bit rates.

Keywords: *image compression; image interpolation; color filter array (CFA); all phase biorthogonal transform (APBT); JPEG*

1. Introduction

As we know, most digital cameras use a single sensor and a color filter array (CFA) to obtain color image information. Through the array, each pixel of the sensor only records one color component, and the full color image can be achieved by interpolation to the obtained data. In various structures of CFA, Bayer pattern [1] is the most popular format, which is more suitable for the color sensitivity of human eyes.

Since each pixel and its adjacent pixels in space are not continuous for Bayer image, the high frequency component is large between the adjacent components. The effect of direct compression to the Bayer image is poor, and the compression ratio is not high enough. Therefore, many lossless and lossy compression algorithms have appeared for such features of the Bayer image. Ref. [2] proposed the "geometric rotation" compression method, and the image data is firstly transformed from RGB space into YCbCr space. Then the Y component after rotation, Cb component and Cr component are compressed by JPEG compression. Ref. [3] adopted integer wavelet transform and Golomb-Rice encoding to compress the CFA data, and better results were achieved. In recent years, Ref. [4] proposed two new lossy compression algorithms, referred to as "structure conversion" and "structure separation". The captured CFA data is compressed by DCT-based JPEG algorithm before full color interpolation, and the algorithm based on structure separation has achieved better performance. However, DCT is still not the optimal choice in image transform coding. One of

ISSN: 2005-4254 IJSIP

its shortcomings is the more complex quantization table; in particular, adjusting the bit rate requires more complex multiplications. Furthermore, block DCT transform coding exists serious blocking artifacts at low bit rates.

To solve the above problems, the all phase biorthogonal transform (APBT) was proposed in [5], which had been applied to still image compression. On the basis of APBT theory, a novel Bayer patterned compression algorithm based on APBT-JPEG and interpolation is proposed in this paper. In the compression step, APBT is adopted instead of the conventional DCT, and the uniform quantization interval is applied instead of the complex quantization table correspondingly according to the energy analysis of the APBT basis images. In the proposed algorithm, the quantization table is simple, and the computation complexity is also reduced.

In Bayer patterned CFA, the performance of interpolation plays a significant role to reconstruct the full color image. Ref. [6] made a comparative study of various interpolation methods, and a comprehensive comparison of the color interpolation algorithms was done in [7]. Based on the previous work, four kinds of interpolation methods, nearest neighbor interpolation, bilinear interpolation [8], cubic convolution interpolation [9] and the all phase IDCT (APIDCT) [10] are discussed in this paper. Experimental results show that the APIDCT interpolation performs close to the conventional methods and behaves better than them at high bit rates.

The rest of this paper is organized as follows. Section 2 introduces the Bayer patterned image compression based on structure separation and DCT-JPEG. In Section 3, the all phase biorthogonal transform, energy analysis of basis images, APBT-JPEG image coding algorithm, and the proposed algorithm for Bayer patterned CFA is presented. Section 4 introduces four interpolation methods: nearest interpolation, bilinear interpolation, cubic convolution interpolation, and the APIDCT interpolation. In Section 5, experimental results and comparisons with conventional algorithm are presented. Finally, conclusion and further research are given in Section 6.

2. Bayer Patterned Image Compression Based on Structure Separation and DCT-JPEG

The Bayer patterned image compression algorithm based on structure separation [4] is shown in Figure 1. The first procedure is color space conversion, by which the original data obtained from CFA is converted from RGB space to YCbCr space, and then separating the luminance and chrominance components. After the separation process, the chrominance component is transformed into a kind of loose rectangle, which needed to become a compact one. And the luminance component is a quincunx, this shape will not be compressed directly without structure separation process. Finally the separated luminance and chrominance components are compressed by the JPEG compression algorithm to obtain the compressed data.

After storage or transmission, the compressed data need to be decompressed, that is an inverse operation of the preceding steps. The recovery luminance and chrominance are combined to generate the image data of the YCbCr space and then to convert them into the RGB color space. Full color image is received by CFA interpolation algorithm.

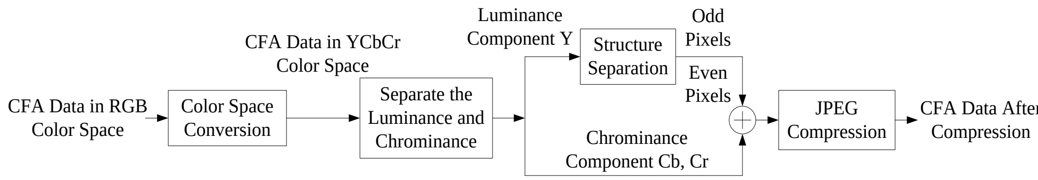

Figure 1. Bayer Patterned Image Compression Algorithm based on Structure Separation

3. Bayer Patterned Image Compression Based on APBT-JPEG

3.1. All Phase Biorthogonal Transform (APBT)

On the basis of all phase digital filtering [11], three kinds of all phase biorthogonal transforms based on the Walsh-Hadamard transform, DCT and IDCT were proposed and the matrices of APBT were deduced in [5]. For example, the elements of $N \times N$ matrix V of the all phase discrete cosine biorthogonal transform (APDCBT) and the all phase inverse discrete cosine biorthogonal transform (APIDCBT) are expressed as Eqs. (1) and (2) respectively.

$$V(i,j)=\begin{cases}\dfrac{N-i}{N^2}, & i=0,1,\cdots,N-1,\ j=0,\\ \dfrac{1}{N^2}\left[(N-i)\cos\dfrac{ij\pi}{N}-\csc\dfrac{j\pi}{N}\sin\dfrac{ij\pi}{N}\right], & i=0,1,\cdots,N-1,\ j=1,2,\cdots,N-1.\end{cases} \tag{1}$$

$$V(i,j)=\begin{cases}\dfrac{1}{N}, & i=0,\ j=0,1,\cdots,N-1,\\ \dfrac{N-i+\sqrt{2}-1}{N^2}\cos\dfrac{i(2j+1)\pi}{2N}, & i=1,2,\cdots,N-1,\ j=0,1,\cdots,N-1.\end{cases} \tag{2}$$

Similar to the DCT matrix, they can be used in image compression transforming the image from spatial domain to frequency domain too.

3.2. Energy Analysis of Basis Images

We define the energy of image matrix as the square of its Frobenius norm, for the decomposited basis image $\boldsymbol{A}_{i,j}=[a_{ij}]$ and the reconstructed basis image $\boldsymbol{B}_{i,j}=[b_{ij}]$, $i,j=0,1,\cdots,N-1$, the energy of basis images can be expressed as

$$E_{\boldsymbol{A}_{i,j}}=\left\|\boldsymbol{A}_{i,j}\right\|_{\mathrm{F}}^2=\sum_{i=0}^{N-1}\sum_{j=0}^{N-1}\left|a_{ij}\right|^2,\ E_{\boldsymbol{B}_{i,j}}=\left\|\boldsymbol{B}_{i,j}\right\|_{\mathrm{F}}^2=\sum_{i=0}^{N-1}\sum_{j=0}^{N-1}\left|b_{ij}\right|^2. \tag{3}$$

When $N=8$, we calculate the energy $E_{\boldsymbol{A}_{i,j}}$ of each decomposited basis image $\boldsymbol{A}_{i,j}$ based on APWBT, APDCBT, and APIDCBT, and the relative energy matrix $\boldsymbol{E}^{\mathrm{d}}$ of the minimum energy after normalization is

$$\boldsymbol{E}^{\mathrm{d}}_{\mathrm{APWBT}}=\begin{bmatrix}4096 & 1344 & 1280 & 576 & 1024 & 320 & 256 & 64\\ 1344 & 441 & 420 & 189 & 336 & 105 & 84 & 21\\ 1280 & 420 & 400 & 180 & 320 & 100 & 80 & 20\\ 576 & 189 & 180 & 81 & 144 & 45 & 36 & 9\\ 1024 & 336 & 320 & 144 & 256 & 80 & 64 & 16\\ 320 & 105 & 100 & 45 & 80 & 25 & 20 & 5\\ 256 & 84 & 80 & 36 & 64 & 20 & 16 & 4\\ 64 & 21 & 20 & 9 & 16 & 5 & 4 & 1\end{bmatrix}, \tag{4}$$

$$\boldsymbol{E}^{\mathrm{d}}_{\mathrm{APDCBT}}=\begin{bmatrix}2166.50 & 858.98 & 660.10 & 486.61 & 338.51 & 215.80 & 118.48 & 46.55\\ 858.98 & 340.57 & 261.72 & 192.93 & 134.21 & 85.56 & 46.98 & 18.46\\ 660.10 & 261.72 & 201.12 & 148.26 & 103.14 & 65.75 & 36.10 & 14.18\\ 486.61 & 192.93 & 148.26 & 109.30 & 76.03 & 48.47 & 26.61 & 10.46\\ 338.51 & 134.21 & 103.14 & 76.03 & 52.89 & 33.72 & 18.51 & 7.27\\ 215.80 & 85.56 & 65.75 & 48.47 & 33.72 & 21.50 & 11.80 & 4.64\\ 118.48 & 46.98 & 36.10 & 26.61 & 18.51 & 11.80 & 6.48 & 2.55\\ 46.55 & 18.46 & 14.18 & 10.46 & 7.27 & 4.64 & 2.55 & 1.00\end{bmatrix}, \tag{5}$$

$$\boldsymbol{E}^{\mathrm{d}}_{\mathrm{APIDCBT}}=\begin{bmatrix}4096.00 & 1759.10 & 1316.50 & 938.04 & 623.53 & 373.02 & 186.51 & 64.00\\ 1759.10 & 755.44 & 565.40 & 402.85 & 267.78 & 160.20 & 80.10 & 27.49\\ 1316.50 & 565.40 & 423.17 & 301.51 & 200.42 & 119.90 & 59.95 & 20.57\\ 938.04 & 402.85 & 301.51 & 214.82 & 142.80 & 85.43 & 42.71 & 14.66\\ 623.53 & 267.78 & 200.42 & 142.80 & 94.92 & 56.78 & 28.39 & 9.74\\ 373.02 & 160.20 & 119.90 & 85.43 & 56.78 & 33.97 & 16.99 & 5.83\\ 186.51 & 80.10 & 59.95 & 42.71 & 28.39 & 16.99 & 8.49 & 2.91\\ 64.00 & 27.49 & 20.57 & 14.66 & 9.74 & 5.83 & 2.91 & 1.00\end{bmatrix}. \tag{6}$$

From Eqs. (4)~(6), it can be concluded that the relative energy of the decomposited basis image of APBT (except APWBT) decreases with the sequency increasing in the main diagonal direction.

When $N=8$, we calculate the energy $E_{\boldsymbol{B}_{i,j}}$ of each reconstructed basis image $\boldsymbol{B}_{i,j}$ based on APWBT, APDCBT, and APIDCBT, and the relative energy matrix $\boldsymbol{E}^{\mathrm{r}}$ of the minimum energy after normalization is

$$\boldsymbol{E}^{\mathrm{r}}_{\mathrm{APWBT}}=\begin{bmatrix}1 & 4 & 4 & 20 & 4 & 36 & 20 & 84\\ 4 & 16 & 16 & 80 & 16 & 144 & 80 & 336\\ 4 & 16 & 16 & 80 & 16 & 144 & 80 & 336\\ 20 & 80 & 80 & 400 & 80 & 720 & 400 & 1680\\ 4 & 16 & 16 & 80 & 16 & 144 & 80 & 336\\ 36 & 144 & 144 & 720 & 144 & 1296 & 720 & 3024\\ 20 & 80 & 80 & 400 & 80 & 720 & 400 & 1680\\ 84 & 336 & 336 & 1680 & 336 & 3024 & 1680 & 7056\end{bmatrix}, \tag{7}$$

$$\boldsymbol{E}^{\mathrm{r}}_{\mathrm{APDCBT}} = \begin{bmatrix} 1.00 & 2.53 & 3.33 & 4.61 & 6.85 & 11.29 & 21.96 & 53.96 \\ 2.53 & 6.40 & 8.42 & 11.66 & 17.33 & 28.58 & 55.57 & 136.55 \\ 3.33 & 8.42 & 11.08 & 15.34 & 22.80 & 37.59 & 73.10 & 179.62 \\ 4.61 & 11.66 & 15.34 & 21.24 & 31.57 & 52.05 & 101.21 & 248.69 \\ 6.85 & 17.33 & 22.80 & 31.57 & 46.91 & 77.35 & 150.40 & 369.56 \\ 11.29 & 28.58 & 37.59 & 52.05 & 77.35 & 127.54 & 248.00 & 609.38 \\ 21.96 & 55.57 & 73.10 & 101.21 & 150.40 & 248.00 & 482.24 & 1185.00 \\ 53.96 & 136.55 & 179.62 & 248.69 & 369.56 & 609.38 & 1185.00 & 2911.70 \end{bmatrix}, \quad (8)$$

$$\boldsymbol{E}^{\mathrm{r}}_{\mathrm{APIDCBT}} = \begin{bmatrix} 1.00 & 2.33 & 3.11 & 4.37 & 6.57 & 10.98 & 21.96 & 64.00 \\ 2.33 & 5.42 & 7.24 & 10.17 & 15.30 & 25.57 & 51.14 & 149.03 \\ 3.11 & 7.24 & 9.68 & 13.59 & 20.44 & 34.16 & 68.33 & 199.11 \\ 4.37 & 10.17 & 13.59 & 19.07 & 28.68 & 47.95 & 95.90 & 279.46 \\ 6.57 & 15.30 & 20.44 & 28.68 & 43.15 & 72.13 & 144.27 & 420.42 \\ 10.98 & 25.57 & 34.16 & 47.95 & 72.13 & 120.57 & 241.15 & 702.76 \\ 21.96 & 51.14 & 68.33 & 95.90 & 144.27 & 241.15 & 482.30 & 1405.50 \\ 64.00 & 149.03 & 199.11 & 279.46 & 420.42 & 702.76 & 1405.50 & 4096.00 \end{bmatrix}. \quad (9)$$

From Eqs. (7)~(9), it can be concluded that the relative energy of the reconstructed basis image of APBT (except APWBT) increases with the sequency increasing in the main diagonal direction. In other words, the APBT has the attenuation characteristics of the high-frequency coefficients, which can be more suitable for the spectrum distribution of natural signals.

3.3. APBT-JPEG Image Coding Algorithm

Based on the energy analysis of basis images, we know that the APBT has the attenuation characteristics of the high-frequency coefficients. During the transform process, coefficients have different frequency weighted; therefore, instead of the complex quantization table based on the visual characteristics of human eyes in JPEG we adopt the uniform quantization interval to transformed coefficients such that our algorithms are simplified. Experimental results show that it is feasible to do so.

In this paper, a novel image compression algorithm based on APBT is proposed. The diagram of APBT-JPEG is shown in Figure 2. In APBT steps, three different transform matrices can be used, and we call them APWBT-JPEG, APDCBT-JPEG and APIDCBT-JPEG respectively. Substantially the same as basic steps of the DCT-JPEG image compression algorithm, there are only differences in the transform (DCT or APBT) and quantization process (quantization table or uniform quantization).

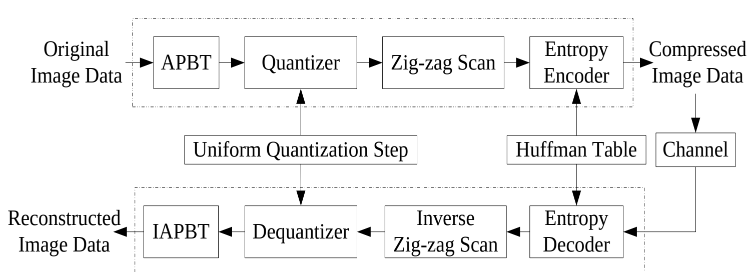

Figure 2. Diagram of the APBT-JPEG Image Compression Algorithm

3.4. The Proposed Algorithm for Bayer Patterned CFA

The Bayer patterned image compression algorithm based on structure separation and APBT-JPEG is shown in Figure 6. In the APBT-JPEG compression step, three different transform matrices can be used. Substantially the same as basic steps of the Bayer patterned compression algorithm based on structure separation, there are only differences in the transform (DCT or APBT) and quantization (quantization table or uniform quantization) steps, as shown in Figure 3.

The first step is color space conversion, by which the original CFA data is converted from RGB space into YCbCr space, and then separate the luminance and chrominance components. After the process of separation, the chrominance component has a kind of loose rectangular shape, which needs to be transformed into a compact rectangular shape. The luminance component is a quincunx, and this shape will not be compressed directly, which needs to be transformed into rectangular shape by structure separation. Finally the separated luminance and chrominance components are compressed by the APBT-JPEG compression algorithm to obtain the CFA data after compression.

After storage or transmission, the compressed data needs to be decompressed, which is an inverse operation of the previous steps. The reductive luminance and chrominance are combined to generate the image data in YCbCr space, which then is converted into the RGB color space data. Finally the full color image is received by CFA interpolation algorithm.

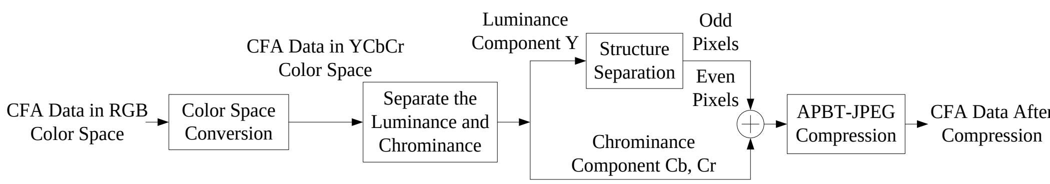

Figure 3. Bayer Patterned Image Compression Algorithm based on Structure Separation and APBT-JPEG

4. Interpolation Methods

4.1. Nearest Interpolation

Nearest interpolation is the earliest grey interpolation algorithm, in which the grey value needed to be interpolated is equal to the grey value of the nearest pixel. The interpolation kernel function is defined as

$$h(x)=\begin{cases}1, & 0\le |x|\le 0.5,\\ 0, & \text{otherwise.}\end{cases} \quad (10)$$

The advantage of nearest interpolation is simple, but it only repeats the nearest grey value, which makes the interpolation effect is not smooth enough and results obvious blocking artifacts.

4.2. Bilinear Interpolation

In mathematics, bilinear interpolation is an extension of linear interpolation for interpolating functions of two variables. The key idea is to perform linear interpolation first in one direction, and then again in the other. Linear interpolation is a first order Lagrange polynomial interpolation using the straight line between the two sampling points to approximate the continuous signal. The interpolation kernel function can be expressed as

$$h(x)=\begin{cases}1-|x|, & 0\le |x|\le 0.5,\\ 0, & \text{otherwise.}\end{cases} \tag{11}$$

The basic idea of bilinear interpolation is to apply the grey values of the four adjacent sampling points to linear interpolation in two directions. Although bilinear interpolation reduces the blocking artifacts to a certain degree, it still makes image detail degradation.

4.3. Cubic Convolution Interpolation

Cubic convolution interpolation [9] is a spatial interpolation method which constructs the interpolation kernel function with the cubic polynomial approximation of sampling function sinc. The interpolation equation can be written as

$$x_a(t)=\sum_{k=-\infty}^{+\infty} x_k g(t-t_k), \tag{12}$$

where x_k are sampled values, $g(t)$ is the interpolation kernel function, and $k\in \boldsymbol{Z}$ is the subscript of sampled points.

Ref. [9] gave the detailed analysis of the cubic interpolation with 4 points information. Several interpolation kernel functions were presented in [6], of which the interpolation kernel function based on 4 points information has the form

$$g_6(x)=\begin{cases}(\alpha+2)|x|^3-(\alpha+3)|x|^2+1, & 0\le |x|<1,\\ \alpha|x|^3+5\alpha|x|^2+8\alpha|x|-4\alpha, & 1\le |x|<2,\\ 0, & \text{otherwise,}\end{cases} \tag{13}$$

where x is the distance between the sampling point and the interpolation point.

4.4. All Phase IDCT Interpolation

Based on the all phase filtering theory [11], the APIDCT filter is proposed in [10]. Let $h_{(2N-1)\times(2N-1)}$ denote the 2-D unit impulse response of the all phase sequency filtering, and $F_{N\times N}$ denote the sequency response vector of length N . Therefore, the design of 2-D APIDCT filter with size of $(2N-1)\times(2N-1)$ is composed of Eqs. (14) and (15)

$$\left[h_{1/4}\right]_{N\times N}=VF_{N\times N}V^{\mathrm{T}}, \tag{14}$$

$$h(m,n)=h(-m,n)=h(m,-n)=h(-m,-n), \tag{15}$$

where $m,n=0,1,\cdots,N-1$, and V denotes the APIDCBT matrix. When $N=4$ and $N=2$, the APIDCT filters used in this paper are

$$h_{7\times7}=\begin{bmatrix} 0 & 0.01 & 0 & 0.01 & 0 & 0.01 & 0 \\ 0.01 & 0 & -0.06 & 0 & -0.06 & 0 & 0.01 \\ 0 & -0.06 & 0 & 0.34 & 0 & -0.06 & 0 \\ 0.01 & 0 & 0.34 & 1 & 0.34 & 0 & 0.01 \\ 0 & -0.06 & 0 & 0.34 & 0 & -0.06 & 0 \\ 0.01 & 0 & -0.06 & 0 & -0.06 & 0 & 0.01 \\ 0 & 0.01 & 0 & 0.01 & 0 & 0.01 & 0 \end{bmatrix}, \tag{16}$$

$$h_{3\times3}=\begin{bmatrix} 0 & 0.25 & 0 \\ 0.25 & 1 & 0.25 \\ 0 & 0.25 & 0 \end{bmatrix}. \tag{17}$$

From Eqs. (16) and (17), it can be seen that the sum of weight coefficients (except the center one) is 1 in each interpolation template and the value of the central symmetric weight coefficients is 0 alternately. In this paper, $h_{7\times7}$ is suitable for G component. When interpolating the R or B component, the APIDCT filters are $h'_{11\times11}$ and $h'_{3\times3}$, which can be obtained by rotating $h_{7\times7}$ and $h_{3\times3}$ 45° respectively. Taking into account the characteristics of the data, the R or B component is firstly interpolated by the filter $h'_{11\times11}$, and then the filter $h'_{3\times3}$ is applied to the obtained data.

5. Experimental Results

In the following experiment, the main work is operated on the basis of APIDCBT-JPEG, and the experimental results show that better performance is achieved.

To measure the performance of algorithm proposed in this paper, we choose the Composite Peak Signal to Noise Ratio (CPSNR) [12] defined as

$$\text{CPSNR}=10\log_{10}\left[\frac{255^2}{\frac{1}{3MN}\sum_{k=1}^{3}\sum_{i=1}^{M}\sum_{j=1}^{N}\left[I_{in}(i,j,k)-I_{out}(i,j,k)\right]^2}\right], \tag{18}$$

where I_{in} and I_{out} are the original and reconstructed images respectively, M and N are the dimensions of each color component array, i and j are the locations of pixels in the color plane, and k represents the color plane.

Table 1 shows the experimental results with the algorithms proposed in Ref. [4] which bilinear is used in the interpolation step and the APBT-JPEG algorithm using the nearest neighbor, bilinear, cubic convolution interpolation and APIDCT interpolation respectively in terms of CPSNR at various bit rates (0.20bpp~1.20bpp).

More clear and intuitive, we draw their rate-distortion curves of image Lena as shown in Figure 4. The reconstructed images Lena obtained by using Ref. [4], nearest neighbor, bilinear, cubic convolution interpolation and APIDCT interpolation at 0.60bpp are presented in Figures 5(a)-(e). From the experimental results, it can be seen that the proposed algorithm outperforms the one based on structure separation in [4]. Moreover, the APIDCT interpolation performs close to the conventional interpolation methods and behaves better than them at high bit rates.

Table 1. CPSNR Comparison of Ref. [4], Nearest, Bilinear, Cubic Convolution and APIDCT Interpolation applied to Image Lena

Bit rate/bpp	Ref. [4] CPSNR/dB	Nearest CPSNR/dB	Bilinear CPSNR/dB	Cubic convolution CPSNR/dB	APIDCT CPSNR/dB
0.20	26.11	25.81	26.77	26.45	26.72
0.30	28.40	27.12	28.59	28.27	28.55
0.40	29.44	27.68	29.62	29.31	29.59
0.50	30.16	28.06	30.35	30.06	30.34
0.60	30.75	28.28	30.89	30.59	30.89
0.80	31.47	28.54	31.65	31.35	31.68
1.00	32.01	28.67	32.16	31.86	32.22
1.20	32.45	28.77	32.50	32.21	32.58

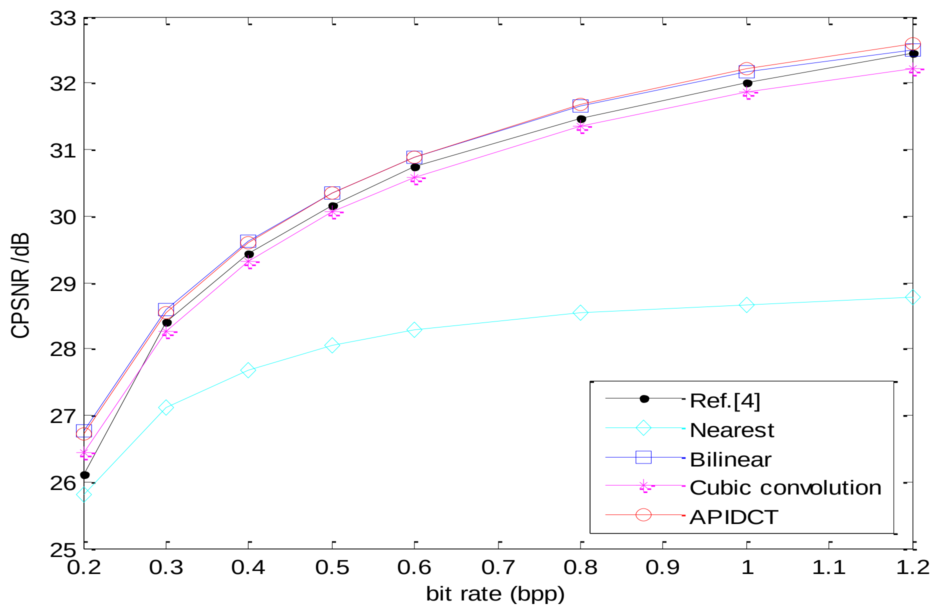

Figure 4. Rate-distortion Curves of Image Lena with Different Interpolation Methods

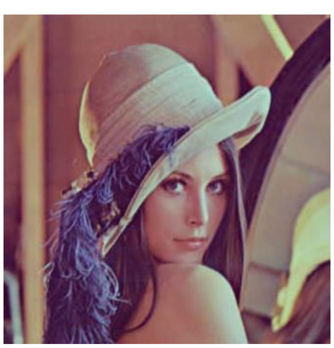

(a)

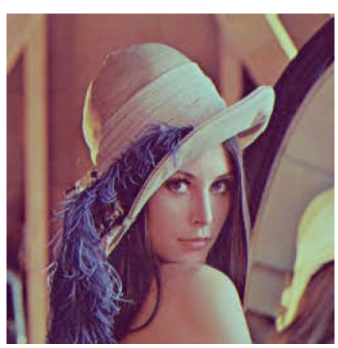

(b)

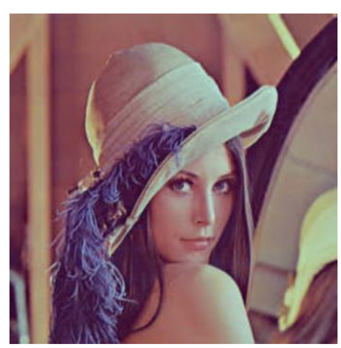

(c)

(d) (e)

Figure 5. Reconstructed Images Lena with Different Interpolation Methods: (a) Ref. [4] with CPSNR = 30.75dB, (b) Nearest with CPSNR = 28.28dB, (c) Bilinear with CPSNR = 30.89dB, (d) Cubic Convolution with CPSNR = 30.59dB, (e) APIDCT with CPSNR = 30.89dB

6. Conclusion

On the basis of the above discussion, it can be concluded that the algorithm based on the APBT-JPEG compression and interpolation is proposed in this paper. In the compression step, the APBT-JPEG replaces the conventional DCT-JPEG, and several interpolation methods are used respectively. Especially according to different characteristics of R, G and B components, different APIDCT filters are applied in the interpolation step. Compared with the conventional algorithms at the same bit rates, experimental results show that the reconstructed image's CPSNR of the proposed algorithm outperforms the one based on structure separation. In addition, the APIDCT interpolation performs close to the conventional methods and behaves better than them at high bit rates. Therefore, the proposed algorithm is more suitable for Bayer patterned image compression.

In this paper, we mainly discussed the scheme based on APBT-JPEG and different interpolation methods for Bayer patterned image compression. Although better performance has been achieved, we didn't consider the optimal design of interpolation methods. Better performance may result by considering variety of post-processing techniques. Furthermore, possibly improvements can be obtained by considering more boundary extension methods at the interpolation step. These issues are left for future research.

Acknowledgements

This work was supported in part by the National Natural Science Foundation of China (Grant No. 61201371). The authors wish to thank Songzhao Xie and Xiaoyan Wang for their help and valuable suggestions to improve the presentation of the paper.

References

[1] B. E. Bayer, "Color imaging array", U.S. Patent, no. 3,971,065, **(1976)** July 20.
[2] S. Y. Lee and A. Ortega, "A novel approach of image compression in digital cameras with a Bayer color filter array", Proceedings of the IEEE International Conference on Image Processing, Thessaloniki, Greece, vol. 3, **(2001)** October 7-10, pp. 482-485.
[3] N. Zhang and X.-L. Wu, "Lossless compression of color mosaic images", IEEE Transactions on Image Processing, vol. 15, no. 6, **(2006)**, pp. 1379-1388.
[4] C.-C. Koh, J. Mukherjee and S.-K. Mitra, "New efficient methods of image compression in digital cameras with color filter array", IEEE Transactions on Consumer Electronics, vol. 49, no. 4, **(2003)**, pp. 1448-1456.

[5] Z. X. Hou, C. Y. Wang and A. P. Yang, "All phase biorthogonal transform and its application in JPEG-like image compression", Signal Processing: Image Communication, vol. 24, no. 10, **(2009)**, pp. 791-802.
[6] T. M. Lehmann, C. Gonner and K. Spitzer, "Survey: interpolation methods in medical image processing", IEEE Transactions on Medical Imaging, vol. 18, no. 11, **(1999)**, pp. 1049-1075.
[7] B. K. Gunturk, J. Glotzbach, Y. Alunbasak, R. W. Schafer and R. M. Mersereau, "Demosaicking: color filter array interpolation", IEEE Signal Processing Magazine, vol. 22, no. 1, **(2005)**, pp. 44-54.
[8] J. Adams, K. Parulski and K. Spaulding, "Color processing in digital cameras", IEEE Micro, vol. 18, no. 6, **(1998)**, pp. 20-30.
[9] R. G. Keys, "Cubic convolution interpolation for digital image processing", IEEE Transactions on Acoustics, Speech, and Signal Processing, vol. 29, no. 6, **(1981)**, pp. 1153-1160.
[10] Z. X. Hou, X. J. Guo and X. Yang, "A novel hierarchical coding algorithm based on multi-subsample and the all phase IDCT interpolation", Proceedings of SPIE Mathematics of Data / Image Coding, Compression, and Encryption VII, with Applications, Denver, CO, USA, vol. 5561, **(2004)** August 4-5, pp. 76-83.
[11] Z. X. Hou and X. Yang, "The all phase DFT filter", Proceedings of the 10th IEEE Digital Signal Processing Workshop and the 2nd IEEE Signal Processing Education Workshop, Pine Mountain, Georgia, USA, **(2002)** October 13-16, pp. 221-226.
[12] J. Mukherjee, M. K. Lang and S. K. Mitra, "Demosaicing of images obtained from single-chip imaging sensors in YUV color space", Pattern Recognition Letters, vol. 26, no. 7, **(2005)**, pp. 985-997.

Authors

Chengyou Wang was born in Shandong province, China in 1979. He received his B.E. degree in electronic information science and technology from Yantai University, China, in 2004 and his M.E. and Ph.D. degree in signal and information processing from Tianjin University, China, in 2007 and 2010 respectively. Now he is a lecturer in the School of Mechanical, Electrical and Information Engineering, Shandong University, Weihai, China. His current research interests include digital image and video processing, wavelet analysis and its applications, and smart grid technology.

Baochen Jiang was born in Shandong province, China in 1962. He received his B.S. degree in radio electronics from Shandong University, China, in 1983 and his M.E. degree in communication and electronic systems from Tsinghua University, China, in 1990. Now he is a professor in the School of Mechanical, Electrical and Information Engineering, Shandong University, Weihai, China. His current research interests include signal and information processing, image and video compression, and smart grid technology.

Hao Yuan was born in Anhui province, China in 1962. She received her B.S. degree in computing technology from Southwest Jiaotong University, China, in 1982 and her M.E. degree in technology of computer application from HeFei University of Technology, China, in 1988. Now she is an associate professor in the School of Mechanical, Electrical and Information Engineering, Shandong University, Weihai, China. Her current research interests include software engineering, smart grid technology and image processing.

